Enhanced Anisotropic Model Building Methodology and Pre-stack Depth Imaging in Deep Water Gulf Of Mexico: A case history

Wilfred Whiteside, Wenlong Xu, Zhiming Li, Ashley Lundy, and Itze Chang, TGS-NOPEC Geophysical Company*

Summary

We present a case study of anisotropic model building and the resulting accuracy of event placement and improved image quality. Approximately 660 OCS blocks of the MC Revival survey located in Mississippi Canyon area were imaged using anisotropic Kirchhoff pre-stack depth migration (Figure 1). The goals of this large scale project were accurate event placement and improved imaging of steep dips, salt boundaries, and subsalt events. To accomplish these goals, all available well information was used to calibrate the seismic velocity model from prior isotropic pre-stack WEM imaging. The resulting vertical velocity model was used to generate isotropic PSDM image gathers for use in determination of the anisotropy parameters epsilon and delta. These fields were derived from an automated two-parameter residual curvature analysis. Multiple iterations of migration for picking salt overhangs were a necessity to properly image salt bases and subsalt events. Focusing of events was enhanced through iterations of tomography both supra and subsalt. We achieved significant improvements in defining the salt boundaries and in positioning the reflectors and salt overhangs by properly accounting for the effect of anisotropy.

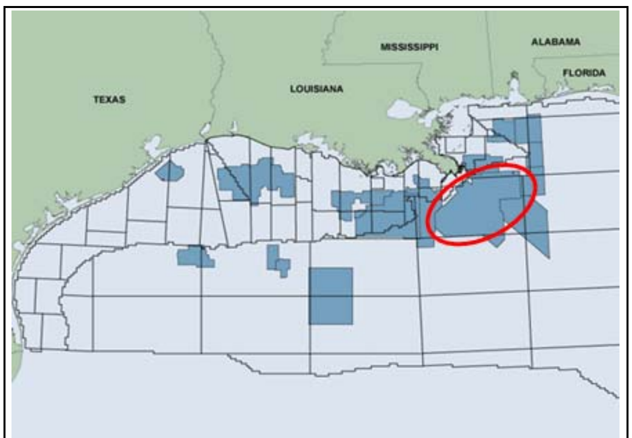

Figure 1: Map showing the location of the survey area.

Introduction

The MC Revival survey is located in an area of the Gulf of Mexico where many deep water discoveries have been made and there is much ongoing exploration activity and interest. The presence of large volumes of salt makes imaging in this region a challenge. Additionally, for exploration work, seismic imaging with accurately positioned events both laterally and vertically is essential. To that end, our goals in this project were to image the region with more accurate event placement, better defined salt boundaries, and better subsalt focusing than previously achieved.

Prior model building and imaging of this survey had been performed using an isotropic wave equation migration (WEM), and an isotropic velocity model. Extensive well log data were available and allowed us to calibrate the isotropic seismic velocities, providing the starting point to our anisotropic model building approach.

Three additional 3-D surveys were prepared to enhance signal-to-noise via swell noise removal and Radon demultiple. Careful matching work was performed to tie the surveys to each other. Additionally, water depth and starting salt surfaces from these surveys were available along with horizons from surrounding 2D data allowing us to form an integrated set of horizons extending out well beyond the imaging area.

Initial Anisotropic Model Building

About 240 checkshots were analyzed in and around the survey area. These were grouped into 30 key well groups. The seismic velocity model from the prior WEM migration was calibrated to generate the initial vertical velocity model, Vz. Typical depthing errors in the isotropically derived starting model ranged from 5% to 12% at a depth of 6,000m with some outliers (Figure 2).

An Isotropic Kirchhoff migration was run on target lines through the key well areas and two-parameter residual curvature scans were run on the resulting image gathers using the residual curvature equation for VTI media shown in equation (1). In VTI media, we can relate migration depth to the true vertical depth and the anisotropy parameters epsilon (ε) and delta (δ) in the following form,

Enhanced Anisotropic Model Building and Imaging

$$Z_M^2(h) = Z_T^2 - \frac{2h^2 z_T^2}{h^2 + z_T^2}\delta - \frac{2h^4}{h^2 + z_T^2}\varepsilon, \qquad (1)$$

where h is offset, and Z_T and Z_M are true depth and migrated depth, respectively, and ε and δ are Thomsen's anisotropy parameters (Alkhalifah, 1997; Sarkar and Tsvankin, 2003). The measured curvature parameters were converted to effective average ε and δ fields. These were then converted to interval ε and δ fields which were smoothed and distributed throughout the model. To verify the fields, the target lines were then anisotropically migrated with the new model. Gather flatness, focusing, and well ties were checked. We made final adjustments and the initial anisotropic sediment model was complete.

Shown in Figure 3 is the previous isotropic WEM image with two well logs posted on the image (gamma ray and sonic logs). The yellow curve indicates the top of a carbonate layer picked on the image. Note that the depth of the top of the carbonate layer was deeper than the top of the layer found in the well logs. The depth error was 610m. The steep salt boundaries were not well focused in the image due to the dip limitation of WEM.

Figure 4 shows the new image obtained by anisotropic Kirchhoff migration using the anisotropic velocity model. Note that the depth of the top of the carbonate layer matches the well depth. In addition, the steep salt flank and overhang of the left-hand side of the salt body are clearly focused in the anisotropic PSDM image.

Velocity Model Updating

The anisotropic sediment model was updated with two passes of grid based tomography. For each of the tomography iterations, 3D anisotropic pre-stack Kirchhoff migration was run with an aperture of 8km and residual curvature analysis was performed on the resulting image gathers. Automatic dip estimation was performed on the stack volume for use in the tomography ray tracing step. Care was taken to mask out rays passing through salt. Vz was updated from the inversion results, and the ε and δ fields were then compensated to preserve well ties.

The salt model was built in four stages due to the need to include salt overhangs in the model. Initially, top of salt was picked on the sediment flood image. At this stage, well salt top depths were checked against the picked top of salt surface. Vz, ε, and δ were then adjusted accordingly in order for salt tops to image at the proper depths. This was done in a manner to preserve resulting image gather flatness.

Base of salt and overhangs were picked after running a top of salt flood iteration of the migration. We then migrated with the initial top and base of salt stamped into the model, and second level top salts were picked on bodies with overhangs. In the final salt model iteration, we flooded the model with top, base, and the second level top of salt horizons. Second level bases were picked, completing the salt phase of model building.

We next migrated the data with the salt model and computed residual curvatures for use in the final tomographic inversion update. The updated regions of the model included both sediment under salt and sediment in regions away from salt. Care was taken not to include deep areas with a higher proportion of remnant multiple energy in the analysis. We updated our model from the inversion results, yielding the final anisotropic velocity model. Changes in Vz matched well with the underlying geology. Shown in Figure 5 is a display of the change in Vz after subsalt tomography on top of the corresponding migrated image. Colors toward the red end of the spectrum indicate a decrease in Vz, and colors toward the blue end indicate an increase in Vz. There is a consistent speedup that occurs near the cretaceous boundary.

The final imaging step was performed with the anisotropic pre-stack Kirchhoff using an increased aperture of 10km and turning rays. Shown in Figure 6 is the isotropic WEM image. The salt model was lacking needed overhangs, and the WEM was not able to capture the steep dips needed to image them. The base of salt is highly curved and unfocused.

Figure 7 shows the final anisotropic image utilizing the new anisotropic velocity model. The steep salt overhangs are imaged significantly better on both sides of the salt body, and the base of salt is quite flat and well focused. Additionally, the sediment truncation against the salt is much better defined than in the WEM.

Conclusions

The combination of a well tying anisotropic sediment model, anisotropic pre-stack Kirchhoff migration, modeling of salt bodies with overhangs, and iterations of both supra and subsalt tomography was applied on a regional scale. The finalized seismic image volume placed events with a much higher degree of accuracy than previous work and resulted in significantly improved image quality. Salt boundaries and steep or overturned events were brought out that previously were inferior or failed to image, and deep and subsalt events were better focused and more continuous.

Acknowledgments

The authors would like to thank their colleagues Simon Baldock and Elizabeth Beal for their help with noise reduction, and to Laurie Geiger, Quincy Zhang, Li Li, Michael Sheaf, and Fatmir Fezga for their valuable contributions during the various phases of model building, and to TGS-NOPEC for their support and release of the material for publication. We also thank Young Kim, Duryodhan Epili, and Chuck Mason for reviewing the manuscript.

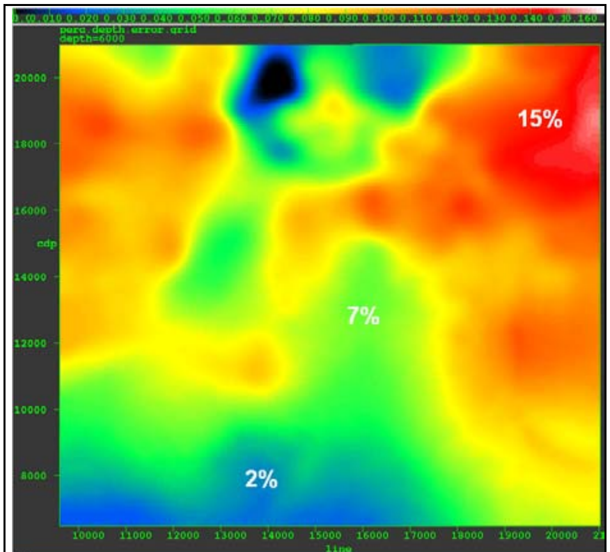

Figure 2: Fractional Depthing Errors of Isotropic Model at 6,000m Depth

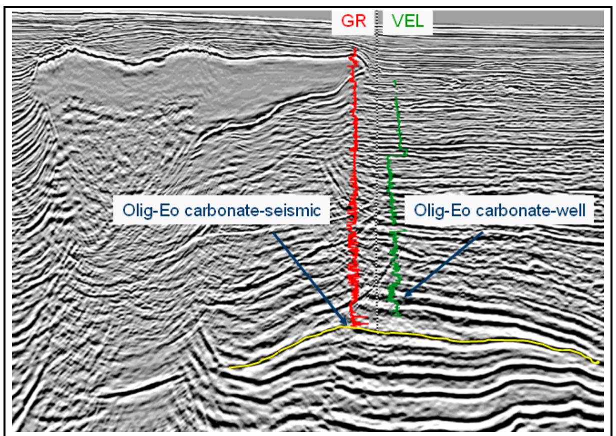

Figure 3: Improper Depthing of Key Layer in Isotropic WEM

Note: GR=gamma ray log, VEL=sonic log

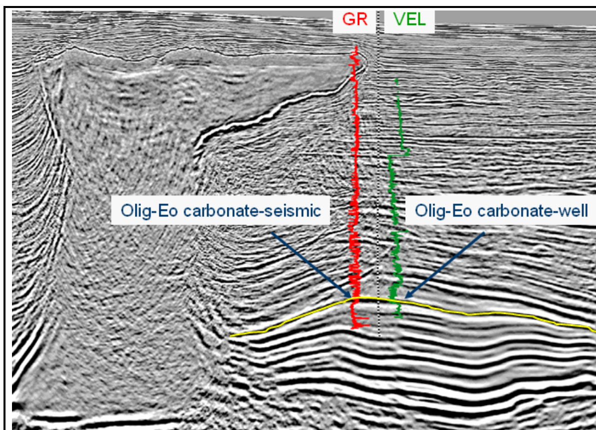

Figure 4: Proper Depthing of Key Layer in Anisotropic KDMIG

Note: GR=gamma ray log, VEL=sonic log

Enhanced Anisotropic Model Building and Imaging

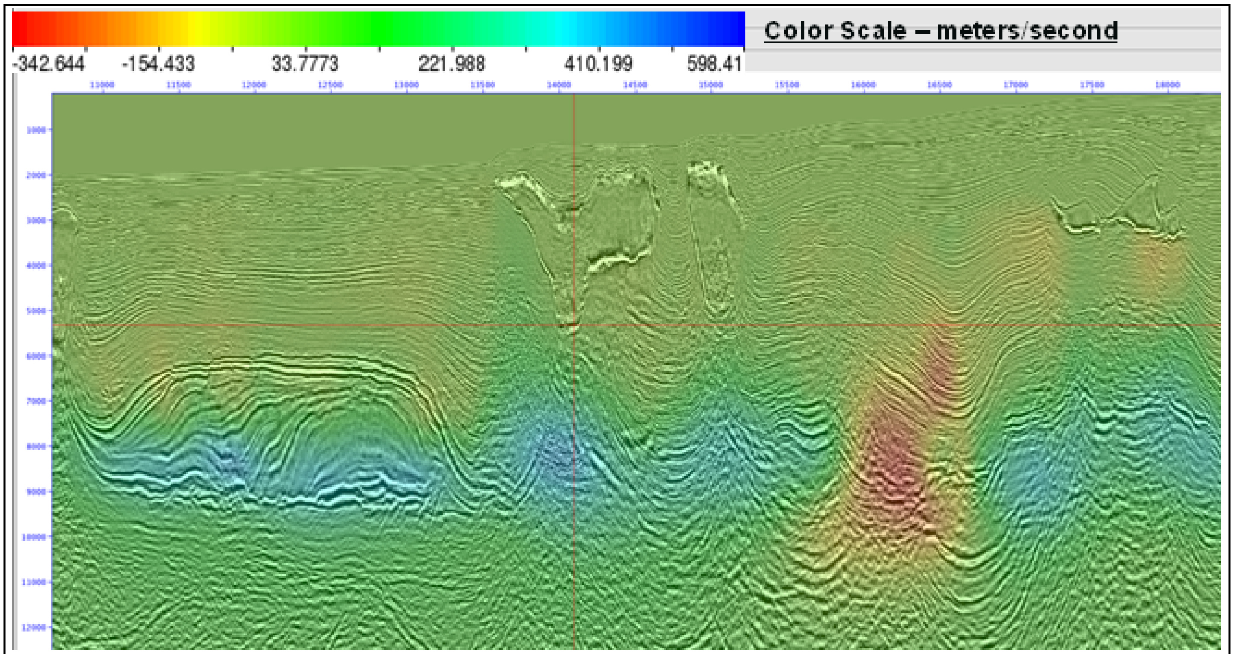

Figure 5: Subsalt tomo vertical velocity update field overlaying anisotropic KDMIG

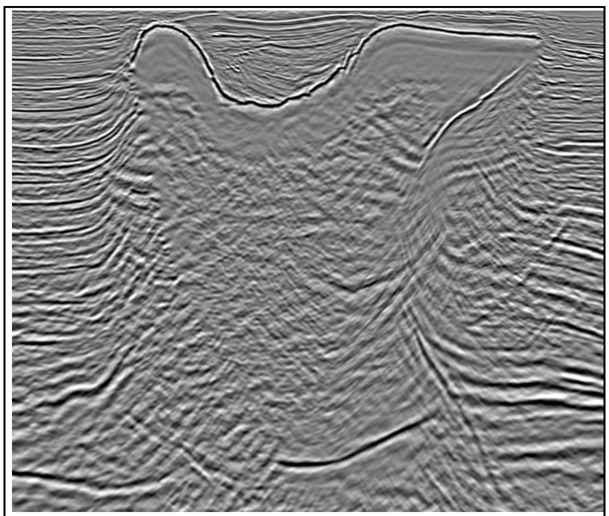

Figure 6: Isotropic WEM without salt overhangs in the model and missing steep and overturned events

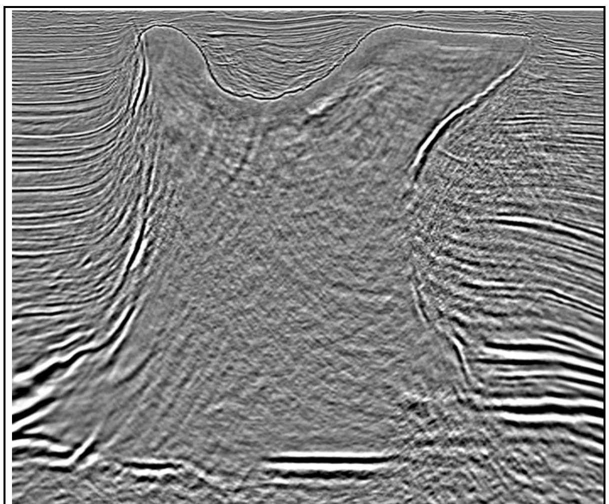

Figure 7: Anisotropic KDMIG with salt overhangs in the model and imaging steep and overturned events

EDITED REFERENCES

Note: This reference list is a copy-edited version of the reference list submitted by the author. Reference lists for the 2008 SEG Technical Program Expanded Abstracts have been copy edited so that references provided with the online metadata for each paper will achieve a high degree of linking to cited sources that appear on the Web.

REFERENCES

Alkhalifah, T., 1997, Velocity analysis using nonhyperbolic moveout in transversely isotropic media: Geophysics, **62**, 1839–1854.

Bear, L. K., T. A. Dickens, J. R. Krebs, J. Liu, and P. Traynin, 2005, Integrated velocity model estimation for improved positioning with anisotropic PSDM: The Leading Edge, **24**, 622–626.

Reshef, M., and R. Murray, 2006, VTI anisotropic corrections and effective parameter estimation after isotropic prestack depth migration: Geophysics, **71**, D35–D43.

Sarkar, D., and I. Tsvankin, 2003, Analysis of image gathers in factorized VTI media: Geophysics, **68**, 2016–2025.